NUMERICAL MODELING OF STREAM-AQUIFER SYSTEMS

Marian Kemblowski

ABSTRACT

In this report we present a new technique for modeling stream-aquifer systems. Modeling procedure consists of simultaneous solution of the Manning equation for open channel flow and the Boussinesq equation descriptive of two-dimensional transient groundwater flow, coupled by an expression for flow across a stream-aquifer interface. Asymmetrical finite difference method is utilized in the numerical solution algorithm.

The model can simulate steady state or unsteady, confined or unconfined groundwater flow. It is also possible to compute quasi three-dimensional groundwater movement (i.e., flow in multi-layered aquifers). Special procedures have been developed for simulating radial flow and flow through a stream-aquifer boundary.

THEORETICAL BACKGROUND

The equations necessary for the development of the mathematical model of a stream-aquifer system include: 1) a groundwater flow equation, 2) stream discharge and stage equation, 3) equations describing flow across stream-aquifer interface for various hydrogeological conditions. The development of these equations is available in current literature. In this section we present a brief description of the derivation procedure, and identify the types of physical assumptions inherent in the flow equations themselves. Such interaction may help one to recognize the range of problem types which can be solved using this model.

GROUNDWATER FLOW EQUATION

The partial differential equation governing unsteady groundwater flow in a heterogeneous aquifer is given by (Bear, 1972)

$$\frac{\partial}{\partial x}\left(T\frac{\partial h}{\partial x}\right) + \frac{\partial}{\partial y}\left(T\frac{\partial h}{\partial y}\right) + q = S\frac{\partial h}{\partial t} \qquad (1)$$

where:

T = aquifer transmissivity, T = mk [L^2T^{-1}]

h = potentiometric head for a confined aquifer, groundwater level for a phreatic aquifer [L]

q = net groundwater recharge rate per unit area [LT^{-1}]

S = coefficient of storage for a confined aquifer, effective porosity for a phreatic aquifer [L^o]

m = saturated thickness of an aquifer, constant in time for a confined aquifer. For phreatic aquifers m(x,y,t) = h(x,y,t) - b(x,y), where b(x,y) is an elevation of the bottom of an aquifer [L]

k = vertically averaged hydraulic conductivity,

$$k = \int_o^m k(z)\,dz/m \qquad [LT^{-1}]$$

It is of interest to note that the derivation of eq. 1 utilizes the Dupuit approximation (Bear, 1972). This approximation assumes that there is no change of the potentiometric head in an aquifer along the vertical coordinate (i.e., $\frac{\partial h}{\partial z} = 0$. It should be emphasized that this asumption may be considered as a good approximation in regions where the slope of the phreatic surface is indeed small and groundwater flow is essentially horizontal.

However, whenever these conditions are not satisfied, the influence of the vertical component of the flow should be included in the numerical model. This is especially important in the vicinity of partially penetrating streams, rivers, wells, and reservoirs. The method of simulating this influence will be shown in the following sections.

STREAM-AQUIFER INTERFACE

The flow across the stream-aquifer interface depends on the hydraulic head difference between a stream and an adjacent aquifer and on the geometric and hydrogeological properties of the stream and aquifer. In this report, we distinguish two different conditions under which the flow may occur. These conditions are: 1) both streambed and aquifer are homogeneous; stream is partially penetrating the aquifer; and 2) streambed and bank of stream are covered with a silt layer, and there is hydraulic connection between stream water and groundwater.

In these two cases the flow rate is determined by the head difference between stream and aquifer and by a parameter which we call resistivity.

Partially Penetrating Streams

In this section, we consider a partially penetrating stream located above a homogeneous aquifer. The basic idea of calculating the influence of the partial penetration is an additional head loss, which is defined as the difference in the heads between fully penetrating and partially penetrating streams, assuming the same flow rate (Fig. 1). For any shape and any position of the partially penetrating stream, this additional loss of head may be

Figure 1. Fully (a) and partially (b) penetrating streams.

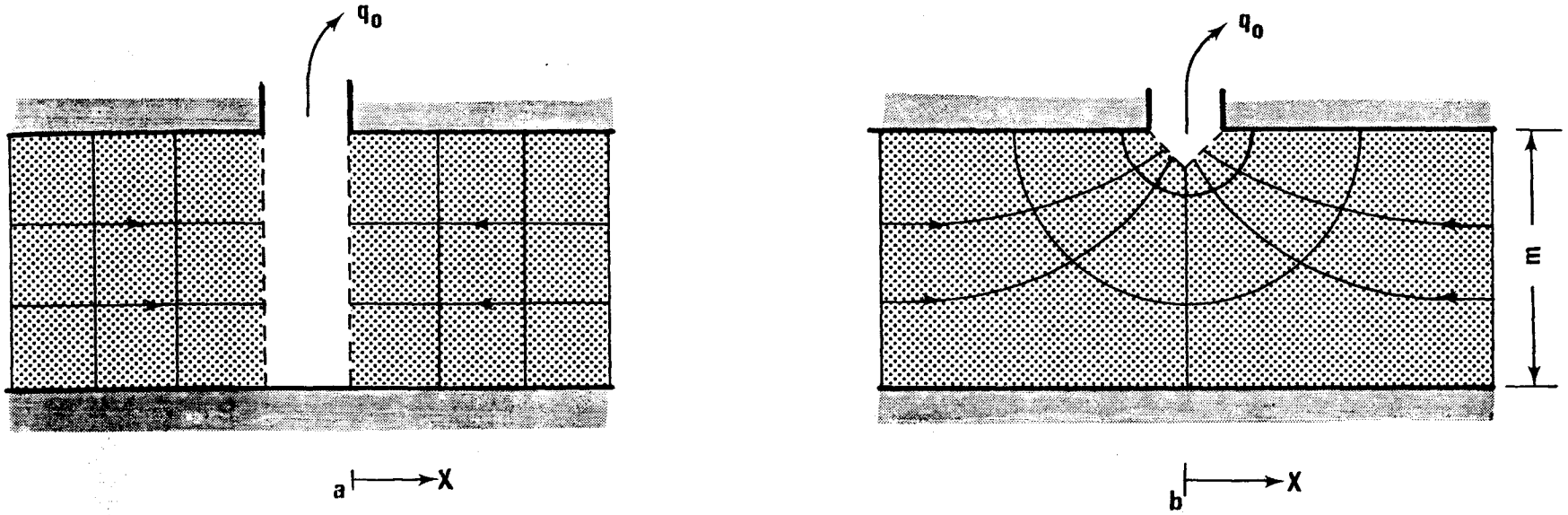

Figure 1

determined by a flow-net analysis. The difference in head at the face of the full, and of the partially penetrating stream of Fig. 1 may be thus estimated by (Huisman, 1972)

$$\Delta s = \frac{1}{2}\frac{q_o}{km}\frac{2}{3}m = \frac{q_o}{k}\frac{1}{3} \qquad (2)$$

Thus, the resistivity in this case is given by

$$R \equiv \frac{\Delta s}{q_o} = \frac{1}{3k} \qquad (3)$$

This additional loss of head corresponds with resistance to flow caused by the convergant flow field.

A formula for the additional loss of head and the resitivity due to partial penetration can be derived only when an easy mathematical description of shape and position of the river is possible. Some examples of hydrogeological schemes, for which the formulae are available, are depicted by Figure 2. The additional drawdown of a half-round stream (Fig. 2a) follows as (Huisman, 1972)

$$\Delta s = \frac{q_o}{\pi k} \ln \frac{m}{\pi r_o} \qquad (4)$$

Thus, resistivity is given by

$$R = \frac{1}{\pi k} \ln \frac{m}{\pi r_o} \qquad (5)$$

Figure 2. Some hydrogeological schemes of partial penetration.

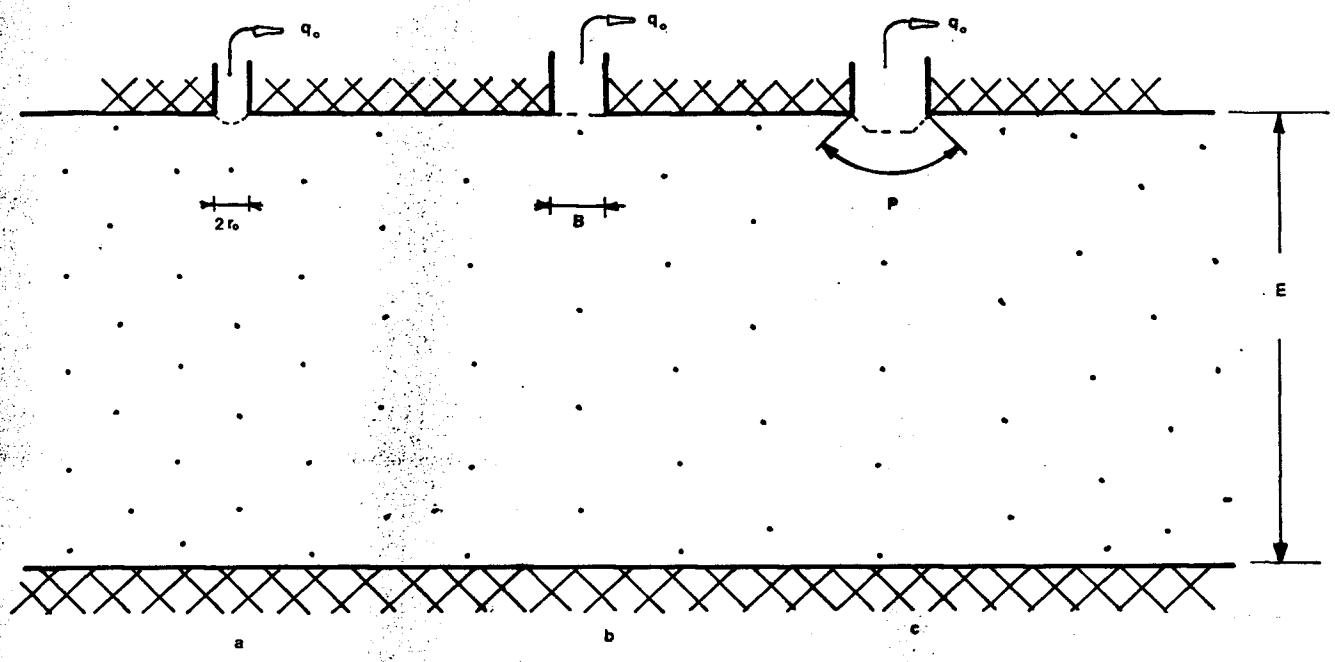

Figure 2

For the rectangular channel located above a confined aquifer in Figure 2b, a mathematical formulation of the additional loss of head and the resistivity may also be given (Huisman, 1972)

$$\Delta s = \frac{q_o}{\pi k} \ell n \ (\sinh \frac{\pi B}{4m}) \tag{6}$$

$$R = \frac{1}{\pi k} \ell n \ (\sinh \frac{\pi B}{4m}) \tag{7}$$

With B small compared to m, this may be simplified to

$$R = \frac{1}{\pi k} \ell n \ (\frac{4m}{\pi B}) \tag{8}$$

Comparison of this formula with the one for the half-round channel shows that with the random shape of Figure 2c, the additional loss of head is given with good approximation by

$$\Delta s = \frac{q_o}{\pi k} \ell n \ (\frac{m}{P}) \tag{9}$$

$$R = \frac{1}{\pi k} \ell n \ (\frac{m}{P}) \tag{10}$$

in which P is the wetted perimeter of the stream. The triangular channel of Figure 1 is drawn with a width of m/3 and a depth m/6. This gives

$$P = \frac{\sqrt{2}}{3} m \tag{11}$$

and as additional loss of head compared with a fully penetrating channel of zero width

$$\Delta s = \frac{q_o}{\pi k} \ln \frac{3}{\sqrt{2}} = 0.22 \frac{q_o}{k} \qquad (12)$$

Compared with the fully penetrating stream of Figure 1 with width m/3 the additional loss of head increases to

$$\Delta s = 0.22 \frac{q_o}{k} + \frac{1}{2} \frac{q_o}{km} = 0.31 \frac{q_o}{k} \qquad (13)$$

in fair agreement with the value of $q_o/3k$ estimated from the flow net analysis.

Shestakow (1965) gives graphs for estimating resistivity of a rectangular channel (Fig. 3). From these curves the resitivity may be estimated with respect to the channel and aquifer geometry and the aquifer hydraulic conductivity. The resistivity is calculated as follows:

$$R = r/k$$

in which r is given by graph 3, and k is the hydraulic conductivity of the aquifer.

Figure 3. Graph for estimating resistivity of a rectangular channel.

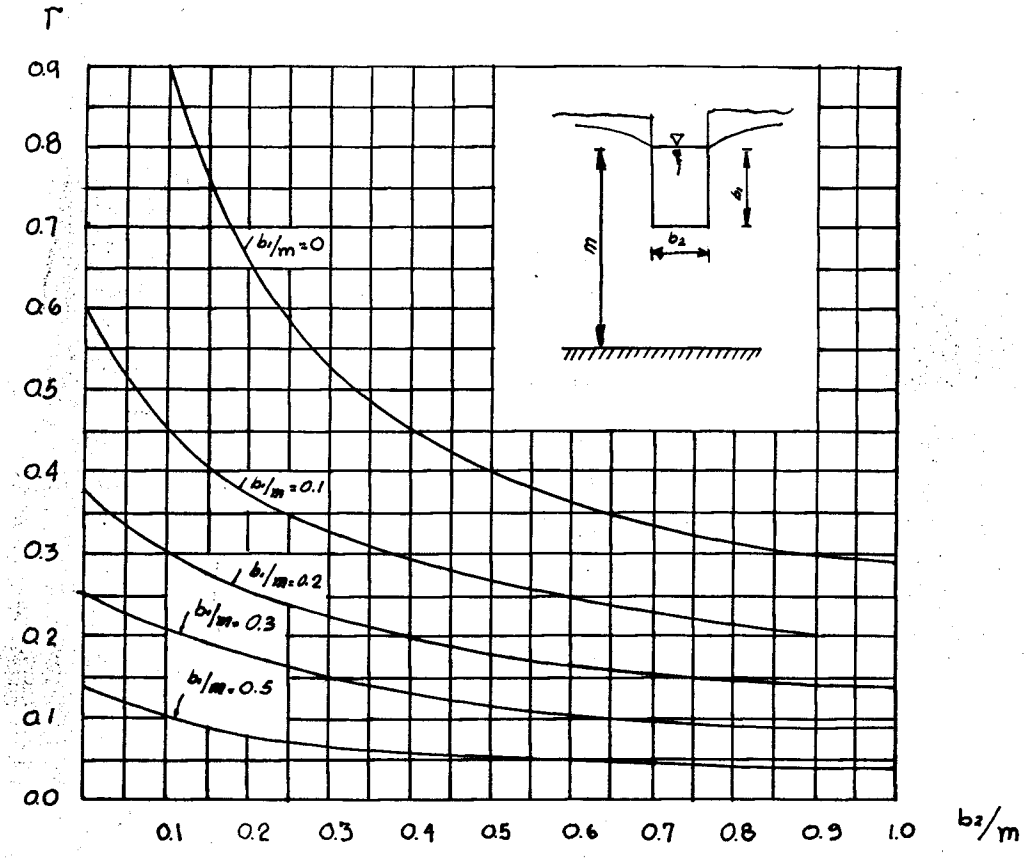
Γ
0.9
0.8
0.7
0.6
0.5
0.4
0.3
0.2
0.1
0.0
b1/m=0
b1/m=0.1
b1/m=0.2
b1/m=0.3
b1/m=0.5
m
b1
b2
0.1
0.2
0.3
0.4
0.5
0.6
0.7
0.8
0.9
1.0
b2/m

Figure 3

Figure 4. Partially penetrating silted stream.

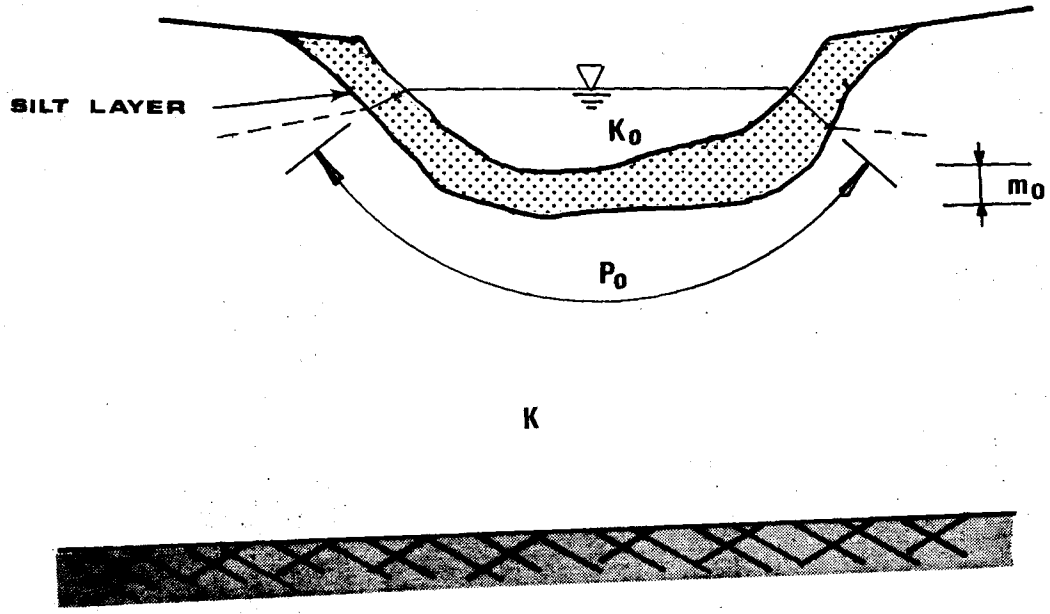

Figure 4

Figure 5. Graph for estimating resistivity caused by stream bed clogging.

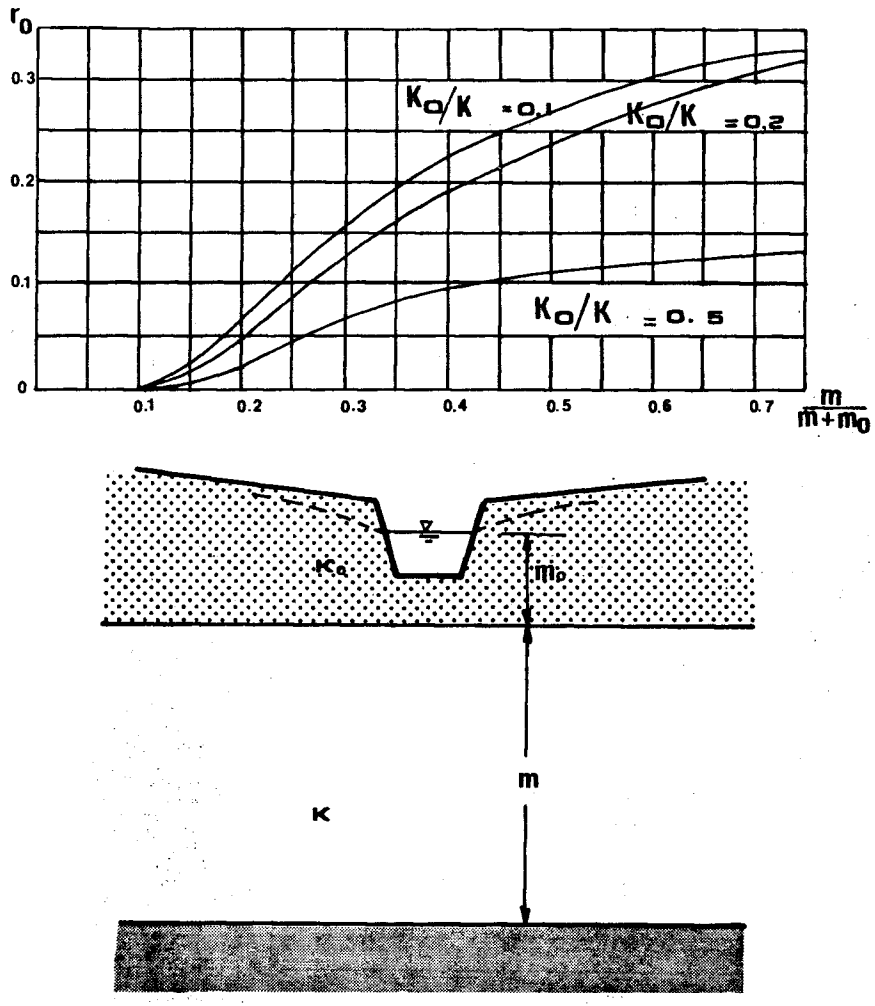
r_0
0.3
0.2
0.1
0
$K_0/K = 0.1$
$K_0/K = 0.2$
$K_0/K = 0.5$
0.1
0.2
0.3
0.4
0.5
0.6
0.7
$\frac{m}{m+m_0}$
K_0
m_0
m
K

Figure 5

clogging layer and aquifer and their hydraulic conductivities. The total resistivity in this case is given by

$$R^* = \left(\frac{m_o}{m} + \frac{k}{k_o}\right) (R + R_o) \qquad (18)$$

in which $R_o = r_o/k$, and r_o is given by graph 5.

It is worthwhile to notice that the best estimation of the total resistivity is obtained from pump tests. The appropriate pump test procedure is described by Walton (1970).

STREAM FLOW EQUATION

Since in this report we consider the unsteady groundwater flow, it would seem logical to use the unsteady channel flow equations known as the Saint-Venant equations to describe stream flow and stage. However, the stream discharge and stage fluctuations ordinarily occur over durations of time that are very short compared to the durations of fluctuations in groundwater flow. Therefore, if one is interested in the long-term influence of groundwater regime upon the stream flow, the steady-state stream flow may be assumed as an approximation (Rovey, 1975).

To represent the relationship between stream discharge and stage the Manning formula was chosen. This formula describes the energy slope due to friction as follows (Chow, 1959)

$$S_f = n^2 \, Q|Q| / (N \, A^2 \, R^{4/3}) \qquad (19)$$

in which

Q = stream discharge $[L^3T^{-1}]$

R = hydraulic radius, $R = A/P$ $[L]$

n = Manning roughness coefficient $[-]$

A = the area of flow $[L^2]$

P = wetted perimeter of the stream $[L]$

N = conversion factor, equal to 1 $m^{2/3}/S^2$ for S.I. units $[L^{2/3}T^{-2}]$

In eq. 19 the unit of length is 1 meter and the unit of time is 1 second. Assuming that stream flow is in steady state and uniform, the energy slope S_f is equal to the channel bed slope S_o (Fig. 6). Thus, we can write

$$Q = A\, R^{2/3} S_o^{1/2}/n \tag{20}$$

The area of flow is assumed to be given by a power law relationship of the form

$$A = az^b + Bz \tag{21a}$$

and likewise

$$P = dz^e + B \tag{21b}$$

where a, b, d and e are empirically determined coefficients, and B is the bottom width of the channel. For a channel of trapezoidal shape (Fig. 6) these relationships are given by

Figure 6. One-dimensional stream flow model. (a) Longitudinal section. (b) Cross section.

a

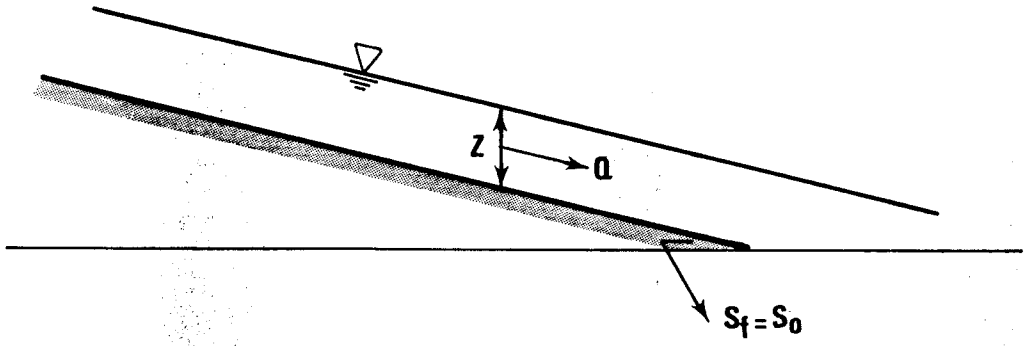

b

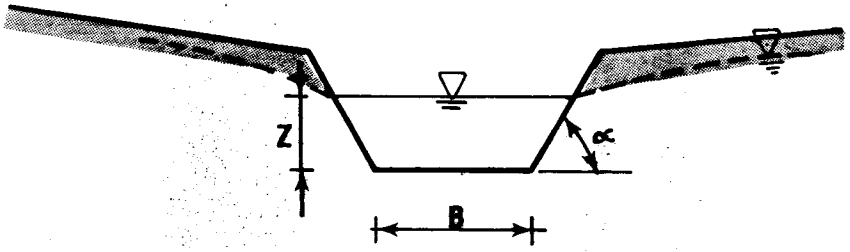

Figure 6

$$A = a_1 z^2 + Bz \tag{22a}$$

and

$$P = 2(1 + a_1^2)^{1/2} z + B \tag{22b}$$

in which a_1 is a reciprocal of the stream bank slope, $a_1 = \mathrm{ctg}\alpha$ (Fig. 6).

Substituting eqs. 21a and 21b in eq. 20 gives

$$Q = (az^b + Bz)[(az^b + Bz)/(dz^e + B)]^{2/3} S_o^{1/2}/n \tag{23}$$

and for a channel of trapezoidal shape:

$$Q = (a_1 z^2 + Bz)[(a_1 z^2 + Bz)/(2(1 + a_1^2)^{1/2} z + B)]^{2/3} S_o^{1/2}/n \tag{24}$$

DEVELOPMENT OF THE SIMULATION MODEL

The basis of the model for simulating flow in a stream-aquifer system is the asymmetrical finite difference method. The application of this method consists of discretizing the study region by an asymmetrical finite difference network and writing the flow balance equation for each nodal point of this network. The interactions between the stream and aquifer are accommodated by imposing additional stream nodes, connected with aquifer nodes below them. The conductivity of this connection depends on hydrogeological conditions, discussed in the earlier section. Inflows and outflows through the upper surface of the model include precipitation, evapotranspiration, irrigation and pumping. The perimeter nodes of the network may be treated as either known

head, or known flux, or known gradient boundary. Computations of river stage as a function of river discharge are performed using the Newton method, simultaneously with groundwater equations. The remainder of this section consists of a description of the methods of modeling radial flow, and quasi three-dimensional groundwater flow. A brief description of the solution procedure appears at the end of this section.

DEVELOPMENT OF THE ASYMMETRICAL FINITE DIFFERENCE METHOD FOR GROUNDWATER FLOW

Finite difference techniques have been used extensively in recent years for solving two-dimensional second order boundary value problems that have proven to be intractable by other methods. The differential equation is replaced by a system of linear (or quasi-linear) equations, whose solution gives the values of the dependent variable at a finite number of node points lying at the intersections of a network. The use of regular polygons, either squares, rectangles, or equilateral triangles, in the formulation of these networks has a desirable property that the equations associated with each node point have a particularly simple, symmetrical form that is identical for all interior points. There are, however, two troublesome problems which arise in connection with the use of regular polygons. The first of them arises when the region has curved boundaries, either external or internal. In such cases some node points near the boundary will be connected to the boundary by network elements of irregular length, thus requiring the use of special equations for these points. The second problem concerns the change of mesh size within the region. It is frequently inefficient from the point of view of computation time to use the same mesh size at all regions. In the areas

where a steeper gradient is expected or near singularities, such as wells, rivers, drains, the mesh size must be reduced if the accuracy of the solution in these areas is to be comparable with the accuracy in parts of the region where the behavior of the dependent function is more uniform. The asymmetrical finite difference method provides means by which the coefficients of a system of algebraic equations can be computed for an arbitrary distribution of node points. The positions of these node points can thus be chosen to fit the boundaries and other special requirements of each problem (Macneal, 1953).

Derivation of Finite Difference Equations

In the method of solution that has been chosen the first step is to connect the chosen points by a network of triangles (Fig. 7). The network should have no cross-overs nor obtuse interior angles.

Consider a portion of this network depicted by Figure 8. The perpendicular bisectors of the sides of the triangles divide the region into polygons surrounding each point. A network of connections is now constructed connecting the vertices of the triangles. The head difference between two points may be interpreted as the line integral of the gradient of the potential (potentiometric) head between these two points

$$h_B - h_A = \int_A^B \nabla h \cdot \vec{d\ell} \qquad (25)$$

The flow in the connection may be interpreted as the total normal flow crossing the common boundary of the polygons surrounding the two points. Since the flux is $-T\nabla h$, we have

Figure 7. Asymmetrical finite difference network.

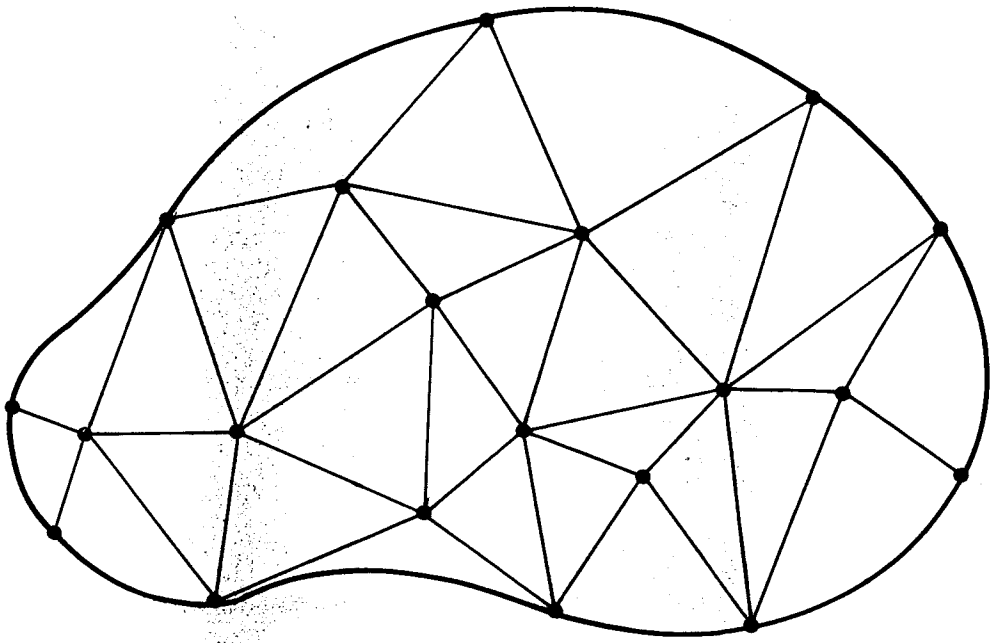

Figure 7

Figure 8. Portion of asymmetrical network.

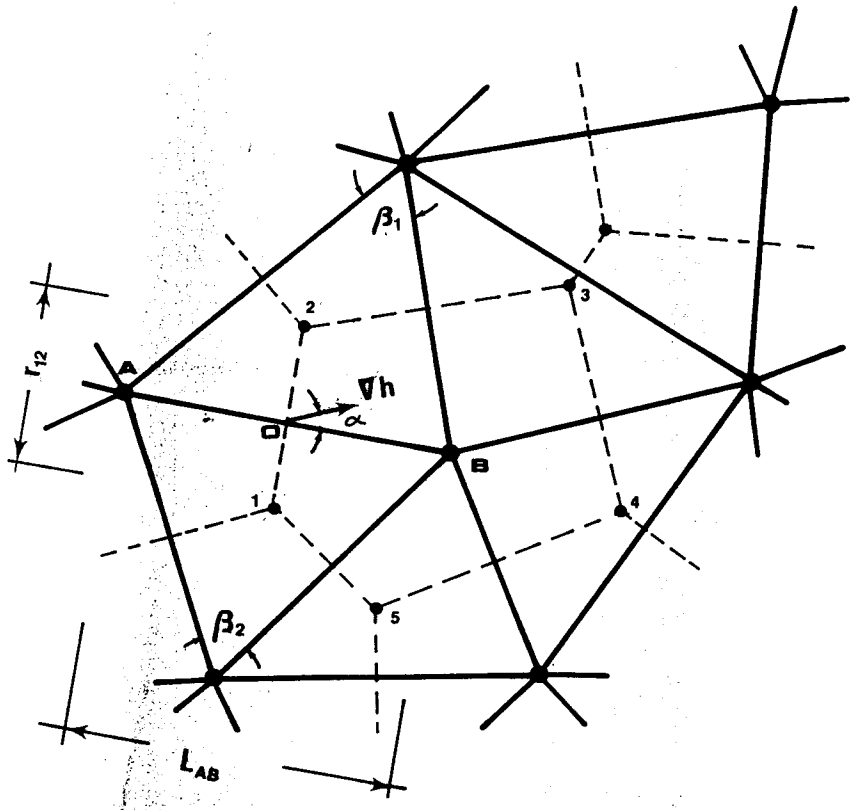

Figure 8

$$Q_{AB} = - \int_{1}^{2} T(\nabla h \cdot \vec{n})\, dr \tag{26}$$

where $\vec{n}$ is a unit normal vector to dr. If ∇h and $T\nabla h$ are now expanded in Taylor's series about the point O (the midpoint of the segment A-B), and all terms except the first are neglected, then

$$h_B - h_A \tilde{=} l_{AB} |\nabla h|_o \cos\alpha \tag{27a}$$

$$Q_{AB} \tilde{=} -T_o\, r_{12}\, |\nabla h|_o \cos\alpha \tag{27b}$$

The value of the conductivity of the connection A-B is

$$J_{AB} \equiv \frac{Q_{AB}}{h_A - h_B} = \frac{T_o\, r_{12}}{l_{AB}} \tag{28}$$

Hence the conductivity J_{AB} depends only on the physical properties of the material and the manner in which region is subdivided. It can also be shown by a simple geometrical argument that (Macneal, 1953)

$$J_{AB} = \frac{T_o}{2} (\mathrm{ctn}\beta_1 + \mathrm{ctn}\beta_2) \tag{29}$$

where β_1 and β_2 are the interior angles of the triangles subtended by the segment AB. If both β_1 and β_2 are acute angles J_{AB} will be physically realizable.

In addition to calculating the value of J_{AB} it is necessary to decide on the area to be associated with the net groundwater recharge term and storage term in eq. 1. If eq. 1 is integrated over the polygon 1-2-3-4-5 surrounding point B of Figure 8.

$$\iint_B \nabla(T\nabla h)\, dB + \iint_B q\, dB - \iint_B S \frac{\partial h}{\partial t}\, dB = 0 \tag{30}$$

by Gauss' integral theorem:

$$\iint_B \nabla(T\nabla h)\, dB = \int_B T(\nabla h \cdot \vec{n})\, dr \tag{31}$$

Hence

$$\int_B T(\nabla h \cdot \vec{n})\, dr + \iint_B q\, dB - \iint S \frac{\partial h}{\partial t}\, dB = 0 \tag{32}$$

If the surface integrals in eq. 32 are replaced by the values of the integrated functions measured at B multiplied by the area of the polygon A_B and the line integral is replaced by network flows from eq. 26, we obtain

$$\sum_p Q_{pB} + q_B A_B - A_B S_B \frac{\partial h}{\partial t}\Big|_B = 0 \tag{33}$$

where Q_{pB} is the flow into node B from p-th adjacent node. If the time derivative is approximated using the central finite difference scheme, and the strictly implicit scheme is utilized for the other terms, the generalized difference equation for node B is obtained:

$$\sum_{p} J_{pB} (h_p^{n+1} - h_B^{n+1}) + q_B^{n+1} A_B - A_B S_B \frac{h_B^{n+1} - h_B^n}{\Delta t} = 0 \qquad (34)$$

where:

J_{pB} = conductivity of the connection p-B $[L^2T^{-1}]$

$$J_{pB} = T_{pB} \frac{r_{pB}}{l_{pB}} \qquad (35)$$

T_{pB} = aquifer transmissivity at the midpoint of the segment p-B $[L^2T^{-1}]$

$$T_{pB} = \frac{m_p + m_B}{2} k_{pB} \qquad (36)$$

k_{pB} = vertically averaged hydraulic conductivity at the midpoint of the segment p-B $[LT^{-1}]$

m_p = saturated thickness of an aquifer at point p [L]

For confined flow

$$m_p = t_p - b_p \qquad (37)$$

For unconfined flow

$$m_p = h_p^{n+1} - b_p \tag{38}$$

t_p = elevation of the top of an aquifer at point p [L]

b_p = elevation of the bottom of an aquifer at point p [L]

h_p^{n+1} = groundwater level (unconfined aquifer) or piezometric head (confined aquifer) at node p for time $(n+1)\Delta t$ [L]

r_{pB} = length of the segment that is common to the polygons surrounding node B and node p [L]

l_{pB} = distance between node p and node B [L]

q_B^{n+1} = net recharge at node B [LT^{-1}]

A_B = the area of the polygon surrounding node B [L^2]

S_B = average effective porosity (unconfined flow) or coefficient of storage (confined) at the polygon surrounding node B [L^0]

Δt = time step [T]

Writing eq. 34 for each node of the network we obtain a system of algebraic equations whose solution gives the values of the unknown variable n(x,y,t) at the nodes for time $(n+1)\Delta t$. These equations are linear for a confined aquifer and non-linear for an unconfined aquifer. For the solution of this system we

use the modified Gauss-Seidel method (Macon, 1963). The interative solution is performed according to the equation

$$h_B^{n+1,k+1} = h_B^{n+1,k} +$$

$$\frac{\sum_p J_{pB}^k (h_p^{n+1,L} - h_B^{n+1,k}) + A_B q_B^{n+1} - \frac{A_B S_B}{\Delta t}(h_B^{n+1,k} - h_B^n)}{\sum_p J_{pB}^k + A_B S_B/\Delta t} \cdot \text{RELAX} \qquad (39)$$

in which

$h_B^{n+1,k+1}$ = the value of the potentiometric head at node B for the iteration step k+1

L = k+1 if p < B

L = k if p > B

RELAX = relaxation coefficient

The relaxation coefficient is constant for the iteration procedure, and has a purpose to accelerate the solution. Its optimum values for confined and unconfined aquifers, found by our numerical experiments, are 1.8 and 1.2, respectively. The iteration procedure continues until the following condition is satisfied

$$\sum_{i=1}^{n} |Res_i| \leq \text{ERROR} \qquad (40)$$

in which

$$Res_i = \sum_p J_{pi}(h_p^{n+1} - h_i^{n+1}) + A_B q_B^{n+1} - \frac{A_B S_B}{\Delta t}(h_B^{n+1} - h_B^n) \qquad (41)$$

and ERROR is the allowed value of the flow non-balance for all nodes at each time step.

Initial and Boundary Conditions

In order to solve the system of equations given by eq. 34, initial and boundary conditions have to be specified. The initial conditions are given by the groundwater level (or piezometric head) values at each node of the network.

In this report we consider three types of boundary conditions: 1) constant head; 2) constant flux; and 3) constant gradient. Over each part of the external boundary of the region one and only one of them has to be defined. In addition the constant head boundary condition may be defined at the interior of the region.

The constant head boundary condition is given by the values of the head at the passive nodes. This value may change in time.

The constant flux boundary condition is given by an additional flow into a boundary node. This additional flow is given by (Fig. 9).

$$Q_A = T_A \frac{\partial h}{\partial n} r_{12} \tag{42}$$

in which T_A = transmissivity at node A, n = unit outward vector normal to the boundary, and r_{12} = length of the segment of the boundary associated with node A. In this case the finite difference equation for node A is

$$\sum_{pA} J_{pA} \left(h_p^{n+1} - h_A^{n+1}\right) + q_A^{n+1} A_A + Q_A - A_A S_A \frac{h_A^{n+1} - h_A^n}{\Delta t} = 0 \tag{43}$$

The constant gradient boundary condition is sometimes specified for unconfined flow. In order to include this condition into the model, we calculate the additional flow Q_A in eq. 43 using formula

$$Q_A = m_A \cdot q_A \tag{44}$$

in which m_A = current aquifer thickness at node A and q_A = flow rate per unit aquifer thickness (Fig. 9)

$$q_A = k_A \frac{\partial h}{\partial n} \cdot r_{12} \tag{45}$$

The value of q_A for constant gradient nodes should be given in input data.

Quasi Three-Dimensional Flow

The type of three-dimensional problem which the computer program can solve is illustrated in Figure 10. The number of layers is limited only by computer storage, since the total number of passive nodes, assuming the same type of boundary conditions for all the layers is equal to the number of nodes in asymmetrical network times the number of layers.

The difference equation for node B of layer 1 in Figure 2 is given by

$$\sum_{p1} J_{p1B1}\left(h_{B2}^{n+1} - h_{B1}^{n+1}\right) + A_B{}_1{}_{B1}^{n+1} - A_B S_{B1} \frac{\left(h_{B1}^{n+1} - h_{B1}^{n}\right)}{\Delta t}$$

$$+k_{B0}\left(h_{B2}^{n+1} - h_{B1}^{n+1}\right) \frac{A_B}{L_{B0}} = 0 \tag{46}$$

Figure 9. Asymmetrical network near boundary.

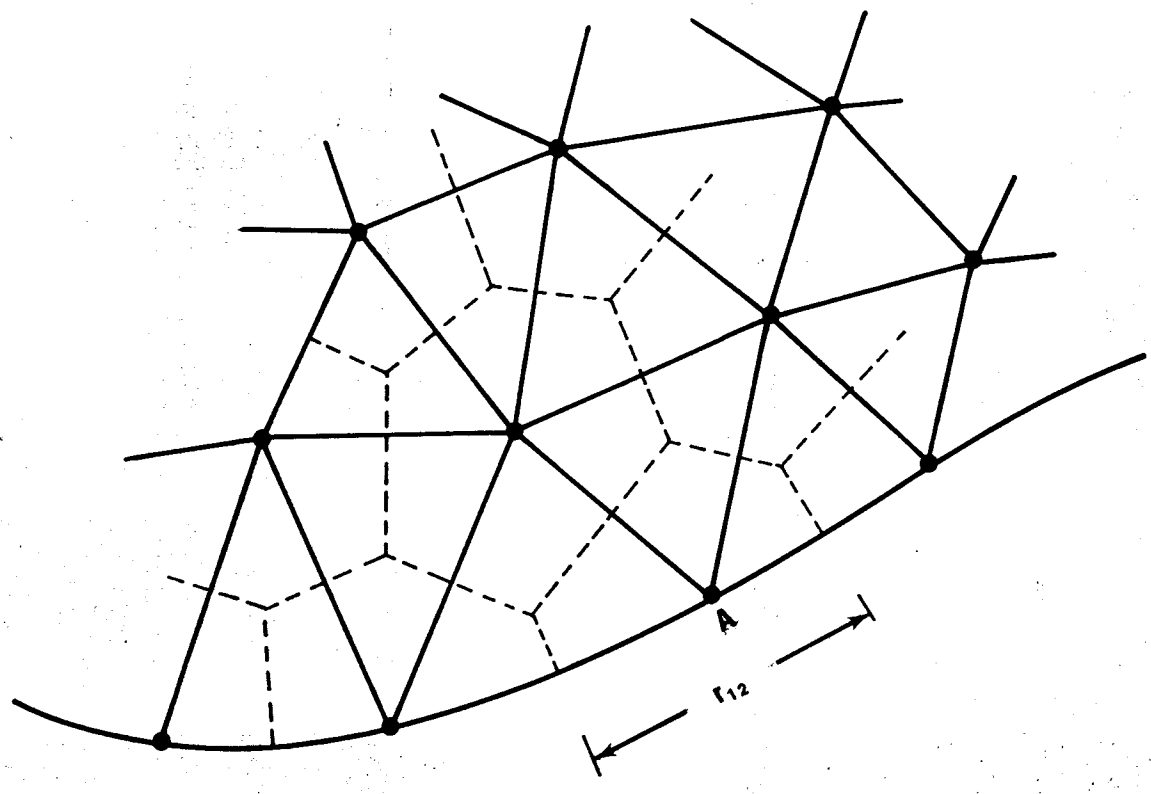

Figure 9

Figure 10. Scheme of three-dimensional groundwater flow.

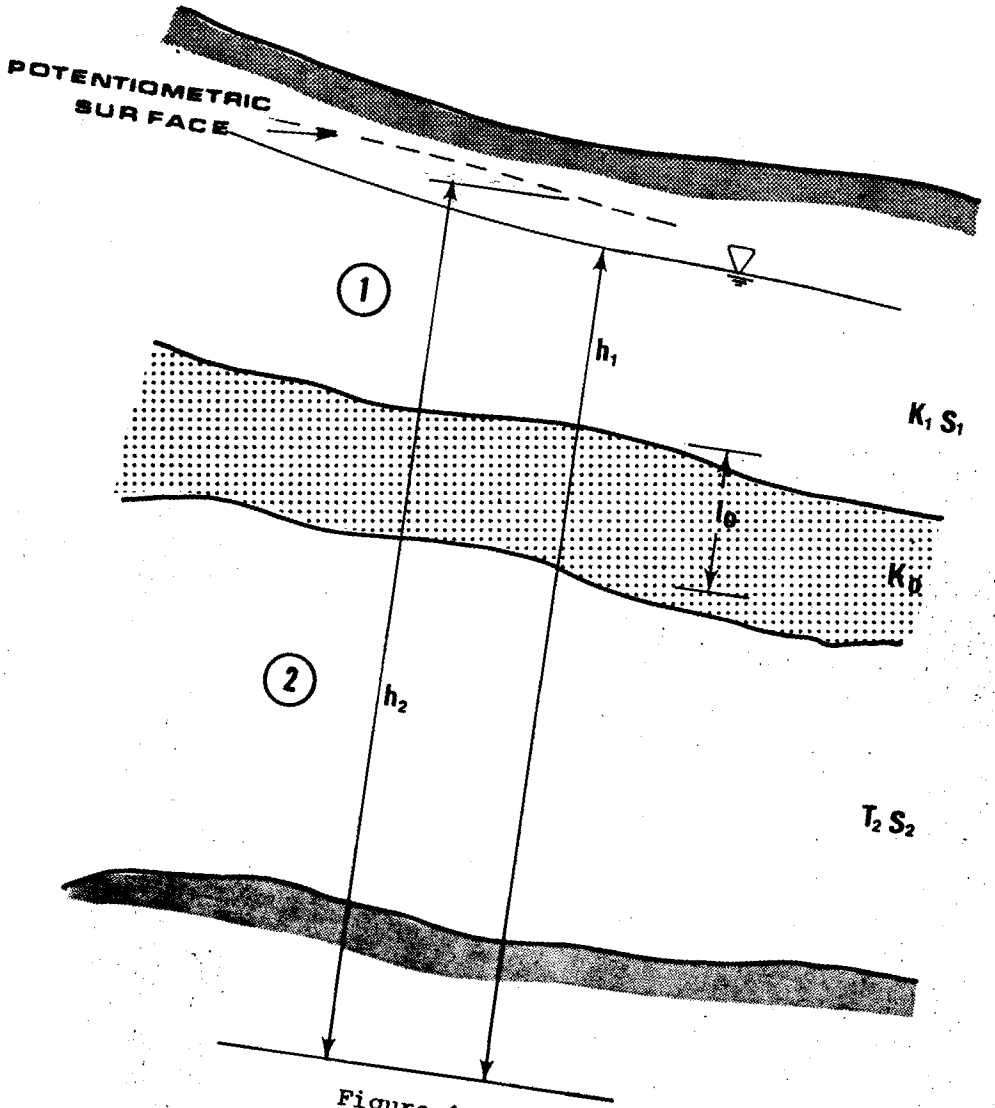

Figure 10

and for node B in layer 2:

$$\sum_{p2} J_{p2B2}\left(h_{p2}^{n+1} - h_{B2}^{n+1}\right) - A_B S_{B2} \frac{\left(h_{B2}^{n+1} - h_{B2}^{n}\right)}{\Delta t}$$

$$+ k_{B0} \left(h_{B1}^{n+1} - h_{B2}^{n+1}\right) \frac{A_B}{L_{B0}} = 0 \qquad (47)$$

in which k_{B0} and L_{B0} are the coefficient of permeability and thickness of semi-impervious layer, respectively. These values should be given as the input data. The value of A_B is calculated by the program itself.

Radial Flow

The linear approximation used in this report does not properly approximate radial flow. In order to calculate radial flow, we will utilize the analytical well equation

$$\Delta S = \frac{Q_o}{2\pi T} \ell n\left(\frac{a}{r_w}\right) \qquad (48)$$

in which ΔS is the difference between the piezometric head at well and the piezometric head at the distance a, and r_w is the well radius.

If we draw around a well a network like one depicted in Figure 11, the flow into the well, according to eq. 28, is given by

$$Q_o = \sum_{i=1}^{8} J_{Bi}^{*} \cdot \Delta s_i = 8 \cdot J_B^{*} \Delta s \qquad (49)$$

Comparing eqs. 48 and 49 we can obtain the expression for the conductivity of the connections around a well

Figure 11. Asymmetrical network near a well.

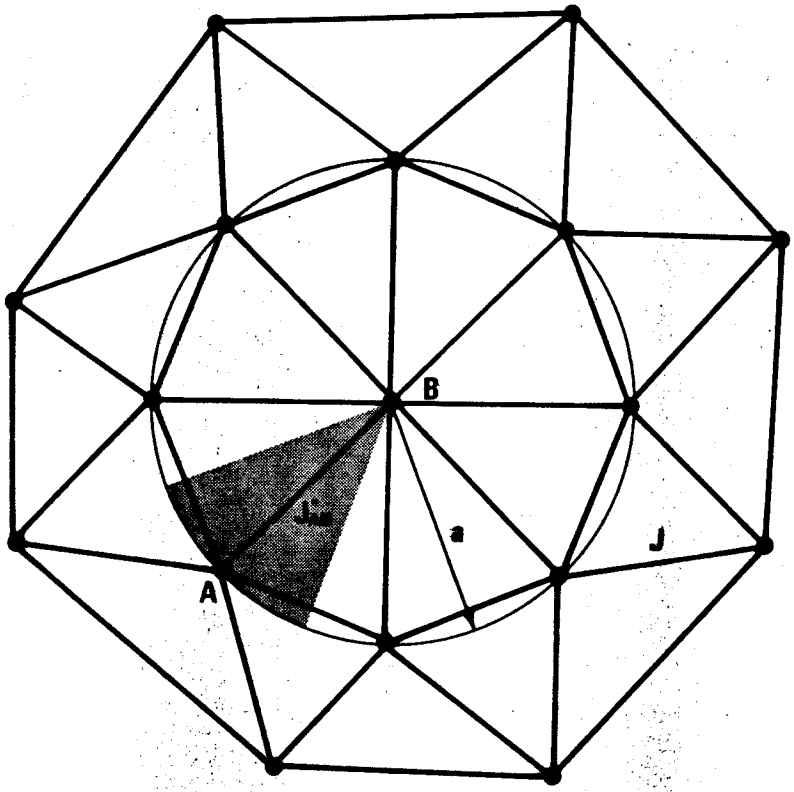

Figure 11

$$J_A^* = \frac{\pi T}{4} \left(\pi n \frac{a}{r_w}\right)^{-1} \tag{50}$$

This conductivity assures agreement between the analytical and numerical solutions.

GROUNDWATER - SURFACE WATER INTERCHANGE

In an earlier section we described the resitivity of stream-aquifer interface against water flow. This resistivity is caused either by partial penetration or by river bed clogging, or by both. In this section we will refer to the total resistivity R*, given by eq. 17. The flow through the stream-aquifer interface is given by

$$q = \Delta h / R^* \tag{51}$$

in which q is the flow per unit length of a strem, R* is a total resistivity, and Δh is the head difference between the stream and an underlying aquifer.

Consider the network depicted by Figure 12. The total flow from aquifer node A to stream node B is given by

$$Q_{AB}^{n+1} = q\, L_A = \left(h_A^{n+1} - h_{Ap}^{n+1}\right) L_A / R_A^* \tag{52}$$

in which L_A is the length of the stream section associated with a river node A_r. Thus, the conductivity of the connection $A\text{-}A_r$ is given by

Figure 12. Numerical network near a stream.

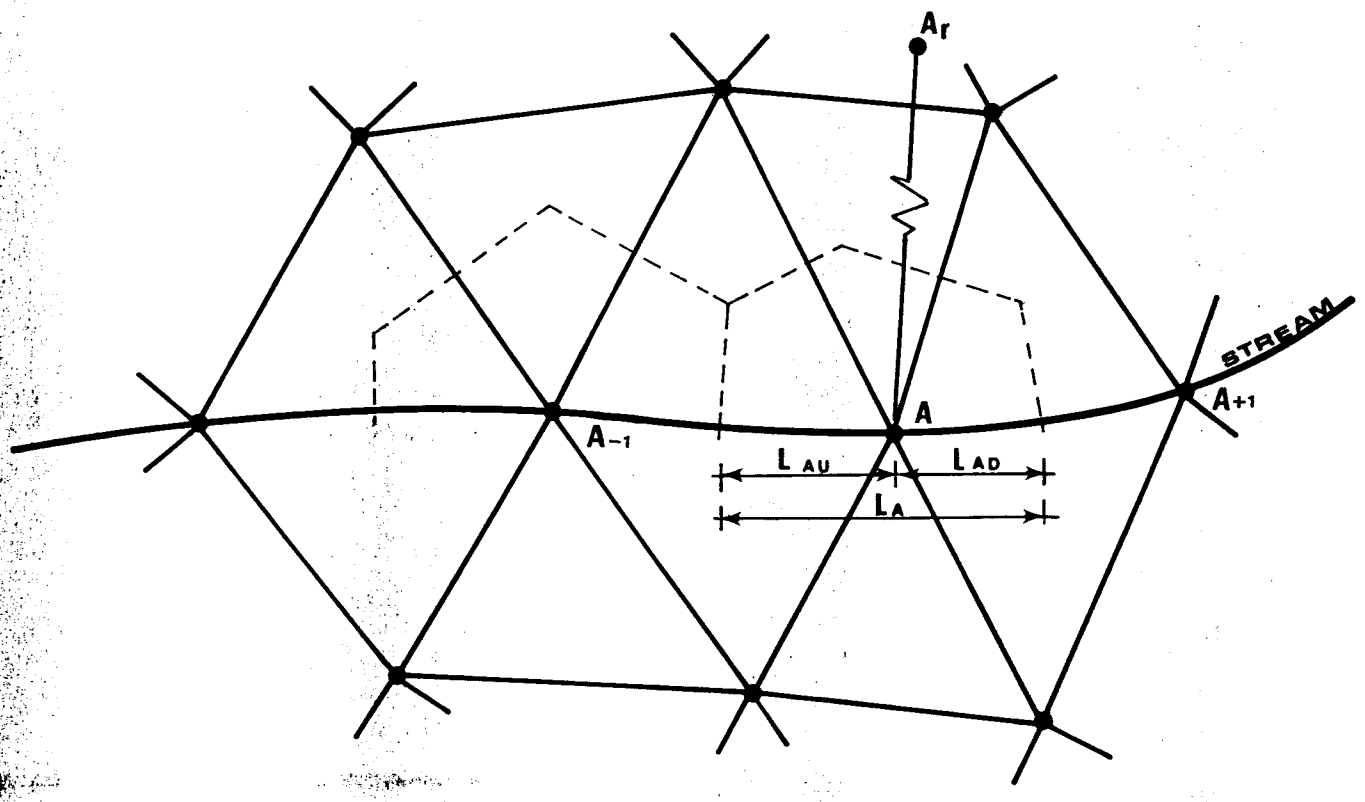

Figure 12

$$J_A = L_A/R_A^* \tag{53}$$

Conductivity calculated this way should be included in the difference equations (eq. 34) of node A and node A_r.

STREAM DISCHARGE AND STAGE CALCULATIONS

Consider the network depicted by Figure 12. Calculation of discharge are initiated at the second node, starting from the upper end, and moved downstream. The discharge at the upper end node is given by the boundary condition. Moving downstream, the discharge at the L-th stream node is computed as

$$Q_L^{n+1} = Q_{L-1}^{n+1} + L_{L-1,D} \cdot Q_{A_1 L-1}^{n+1}/L_{L-1} + L_{L_1 U} \cdot Q_{A_1 L}^{n+1}/L_L \tag{54}$$

in which

Q_L = stream discharge at the L-th stream node

$Q_{A_1 L-1}$ = the flow from an aquifer to the L-1 th node, computed according to eq. 47

$L_{L-1,D}$ = the length of the lower part of the stream section associated with the L-1 th node

$L_{L,u}$ = the length of the upper part of the stream section associated with the Lth node

L_L = the length of the stream section associated with the Lth node

During the iteration procedure, after the discharge at a certain node is calculated, we can update the value of the stream stage; solving eq. 24 for z. This equation is an implicit function of the flow depth z. In order to solve it we will use the Newton method (Macon, 1963). Eq. 24 may be rewritten in equivalent form

$$f(z) = Q - (az^2 + Bz)[az^2 + Bz)/(Cz + B)]^{2\ 3}\ S_o^{1/2}/n = 0 \qquad (55)$$

in which a = ctgα (Fig. 8) and $c = 2(1+a^z)^{1/2}$. A sequence of successive approximations z_1, z_2, z_3, ..., is computed from a starting value z_o by means of the relation

$$z_{i+1} = g(z_i) \qquad i = 1,2,3 \qquad (56)$$

in which

$$g(z) = z - \frac{f(z)}{df(2)/dz} \qquad (57)$$

and

$$\frac{df(z)}{dz} = \frac{1}{3}\ (f(z) - Q) \cdot (5(2az + B)/(az^2 + B2) - 2c/(cz + B)) \qquad (58)$$

The iteration procedure, described by eq. 56, continues until the following condition is satisifed.

$$|f(z)| < 0.01\ Q \qquad (59)$$

NUMERICAL RESULTS

In this section we present results of numerical simulation of two stream-aquifer interaction problems and compare them with the appropriate analytical solutions. Two problems are analyzed: 1) groundwater flow changes as the result of stream stage fluctuations and 2) unsteady groundwater flow to a single well in an aquifer bounded by a recharge boundary.

Groundwater Flow Changes as the Result of Stream Stage Fluctuations

Consider a confined aquifer overlain and underlain by aquicludes and fully penetrated by a stream. The aquifer is homogeneous, isotropic and infinite in areal extent. The partial differential equation governing the one-dimensional flow of groundwater is

$$T \frac{\partial^2 h}{\partial x^2} = S \frac{\partial h}{\partial t} \tag{60}$$

If the stream stage fluctuates as a simple harmonic motion, the boundary conditions may be written as (Walton, 1970)

$$h = h_o + S_o \sin(2\pi t/t_s) \qquad \text{for } x = 0 \tag{61a}$$

$$h = h_o \qquad \text{for } x = \infty \tag{61b}$$

in which h_o is the initial stream stage ($t = 0$), S_o is the amplitude of the stream stage fluctuations, and t_s is the period of the uniform stage change.

For initial condition given by

$$h(x,o) = h_o + S_o \exp[-x(\pi S/t_s T)^{1/2}]\sin[-x(\pi S/t_s T)^{1/2}] \tag{62}$$

eq. 60 has an analytical solution

$$h(x,t) = h_o + S_o \exp[-x(\pi S/t_s T)^{1/2}]\sin[2\pi t/t_s - x(\pi S/t_s T)^{1/2}] \quad (63)$$

which defines a wave motion whose amplitude rapidly decreases with distance x.

The amount of flow into or from the aquifer per unit length of the stream is given by

$$q(t) = T \cdot \frac{\partial h}{\partial x}\Big|_{x=0} = T \cdot I(t) \quad (64)$$

From eq. 63 we can calculate

$$I(t) = S_o \exp[-x \cdot A][-A][\sin(2\pi t/t_s - xA) + \cos(2\pi t/t_s - xA)] \quad (65)$$

in which $A = (\pi S/t_s T)^{1/2}$

In numerical simulation the following values of parameters were used: S_o = 2m, t_s = 2 days, T = 20 m^2/day, S = 0.001, h_o = 0.0 m.

Figures 13-15 show the fluctuations of piezometric head at x = 90 m. the numerical results shown in Figures 13, 14, and 15 were obtained for Δt equal to 0.1 day, 0.05 day, 0.01 day, respectively. The smaller time steps allow better approximation of the stream stage fluctuations, thus improving accuracy of the numerical results.

Figure 13. Numerical and analytical results for the aquifer potentiometric head fluctuations. $x = 90$ m, $\Delta t = 0.1$ day

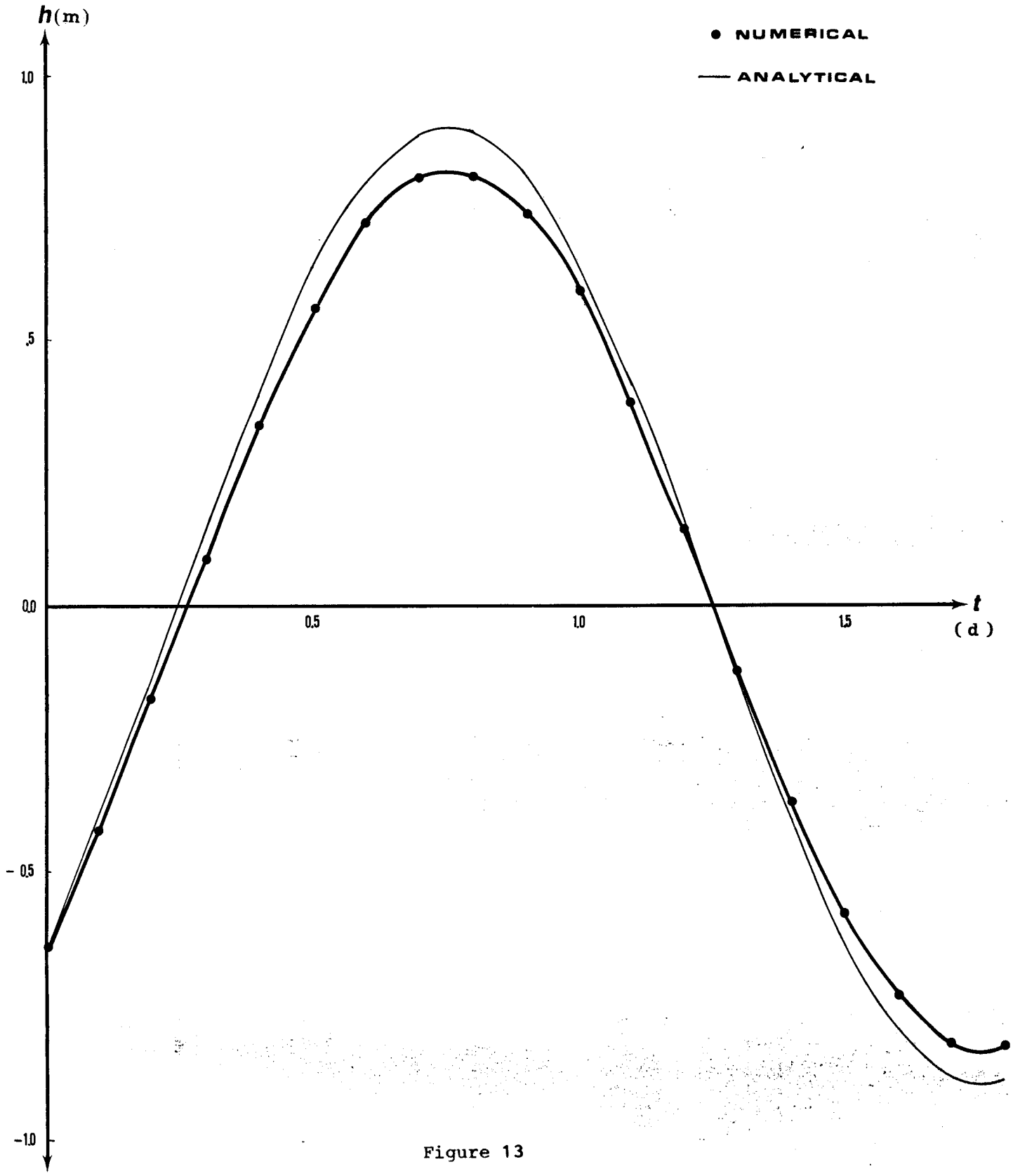

Figure 13

Figure 14. Numerical and analytical results for the aquifer potentiometric head fluctuations. $x = 90$ m, $\Delta t = 0.05$ day.

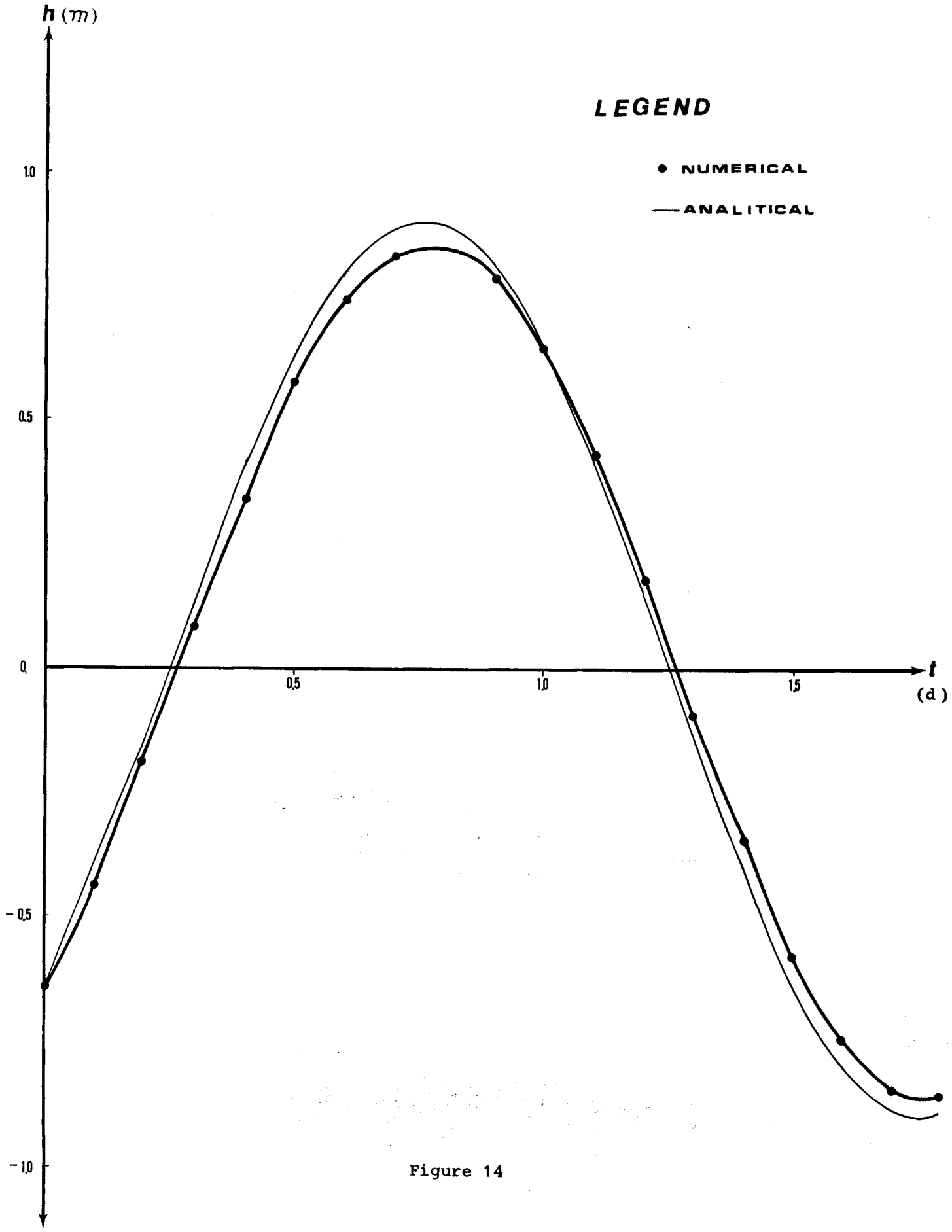

Figure 14

Figure 15. Numerical and analytical results for the aquifer potentiometric head fluctuations. $x = 90$ m, $\Delta t = 0.01$ day.

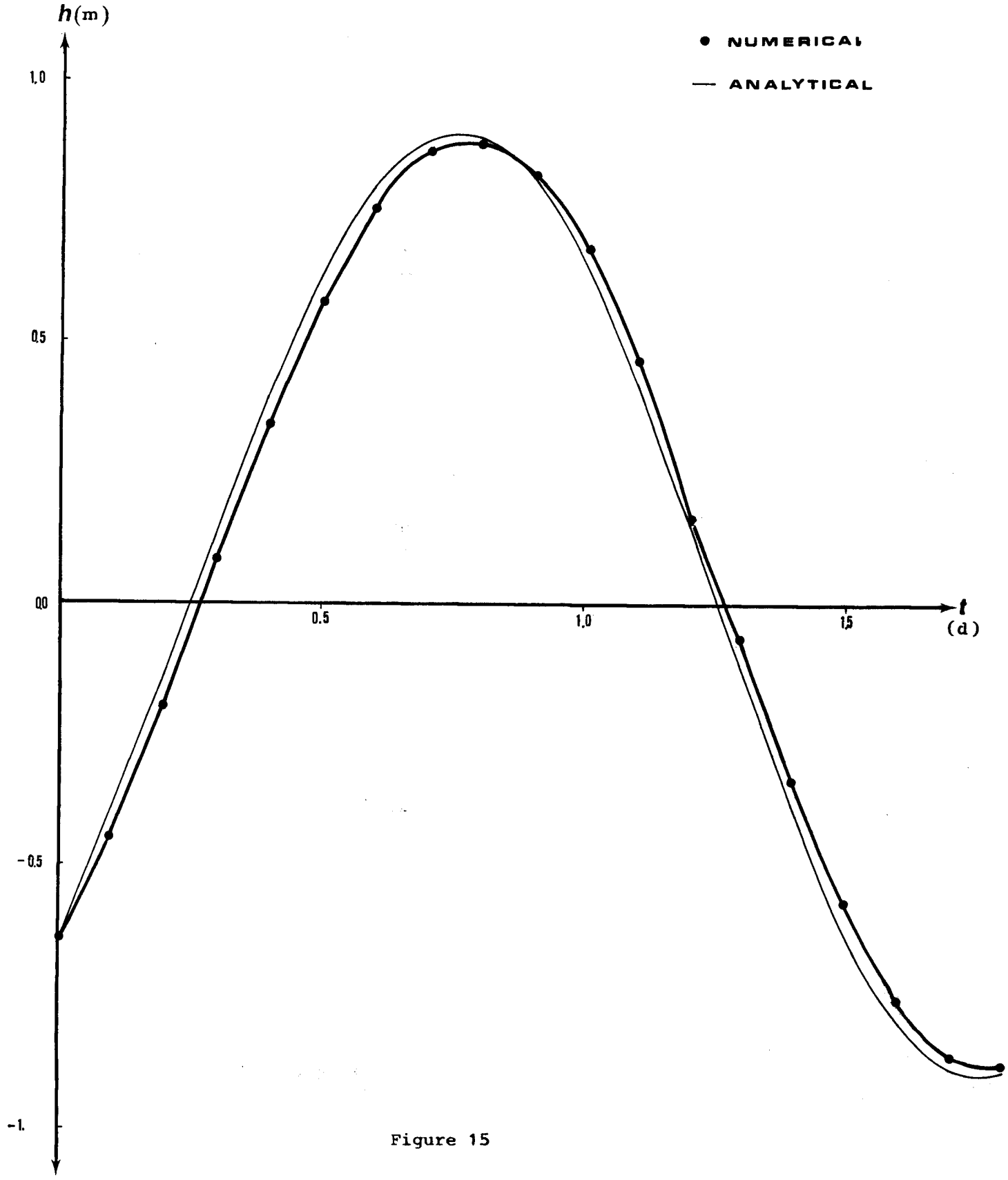

Figure 15

Figure 16 shows analytical and numerical results of the flow into or from the aquifer across the stream-aquifer interface. The numerical results were obtained for $\Delta t = 0.1$ day. It is seen that the numerical results approximate analytical solution with good accuracy.

Unsteady Fow to a Single Well Located Near a Stream

Figure 17 shows a confined aquifer fully penetrated by the stream and well. The aquifer is homogeneous and isotropic, and simi-infinite in areal extent. The differential equation governing the two-dimensional groundwater flow caused by pumping is

$$T \frac{\partial^2 h}{\partial x^2} + T \frac{\partial^2 h}{\partial y^2} + Q = S \frac{\partial h}{\partial t} \tag{66}$$

with initial and boundary conditions given by:

$$\begin{aligned} h(x,y,0) &= h_o \\ h(0,y,t) &= h_o \\ h(x,\pm\infty,t) &= h_o \\ h(\infty,y,t) &= h_o \end{aligned} \tag{67}$$

Using the imaginary well method, we obtain an analytical solution of eq. 66 (Huisman, 1972)

$$h(x,y,t) = \frac{Q}{4\pi T} \left(W(u^2)_{r_r} - W(u^2)_{r_i} \right) \tag{68}$$

Figure 16. Numerical and analytical results for the flow across the stream-aquifer interface, $\Delta t = 0.1$ day.

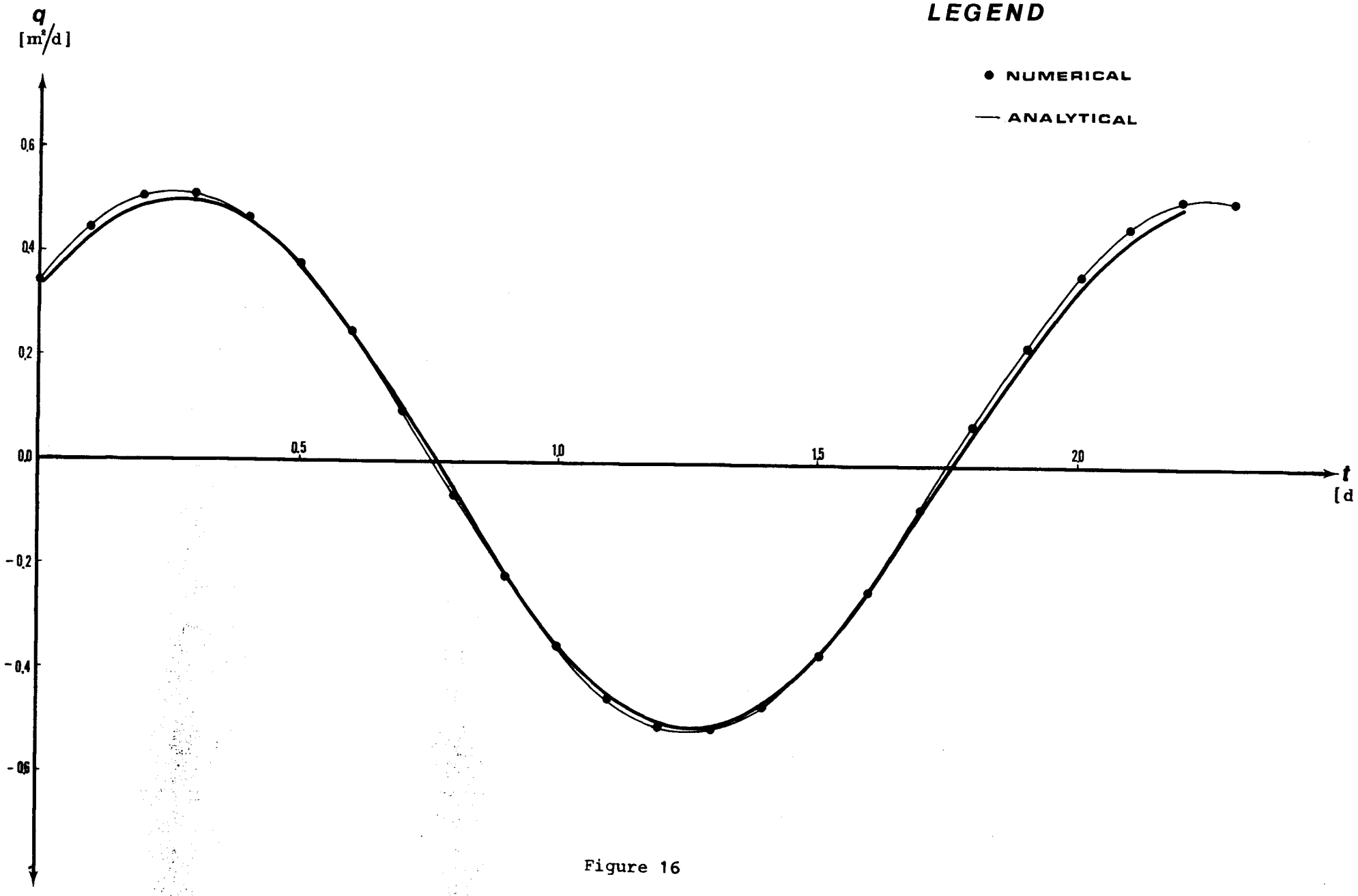
q
[m²/d]
LEGEND
NUMERICAL
ANALYTICAL
0.6
0.4
0.2
0.0
-0.2
-0.4
-0.6
0.5
1.0
1.5
2.0
t
[d

Figure 16

Figure 17. Hydrogeologic scheme of flow to a single well located near a stream.

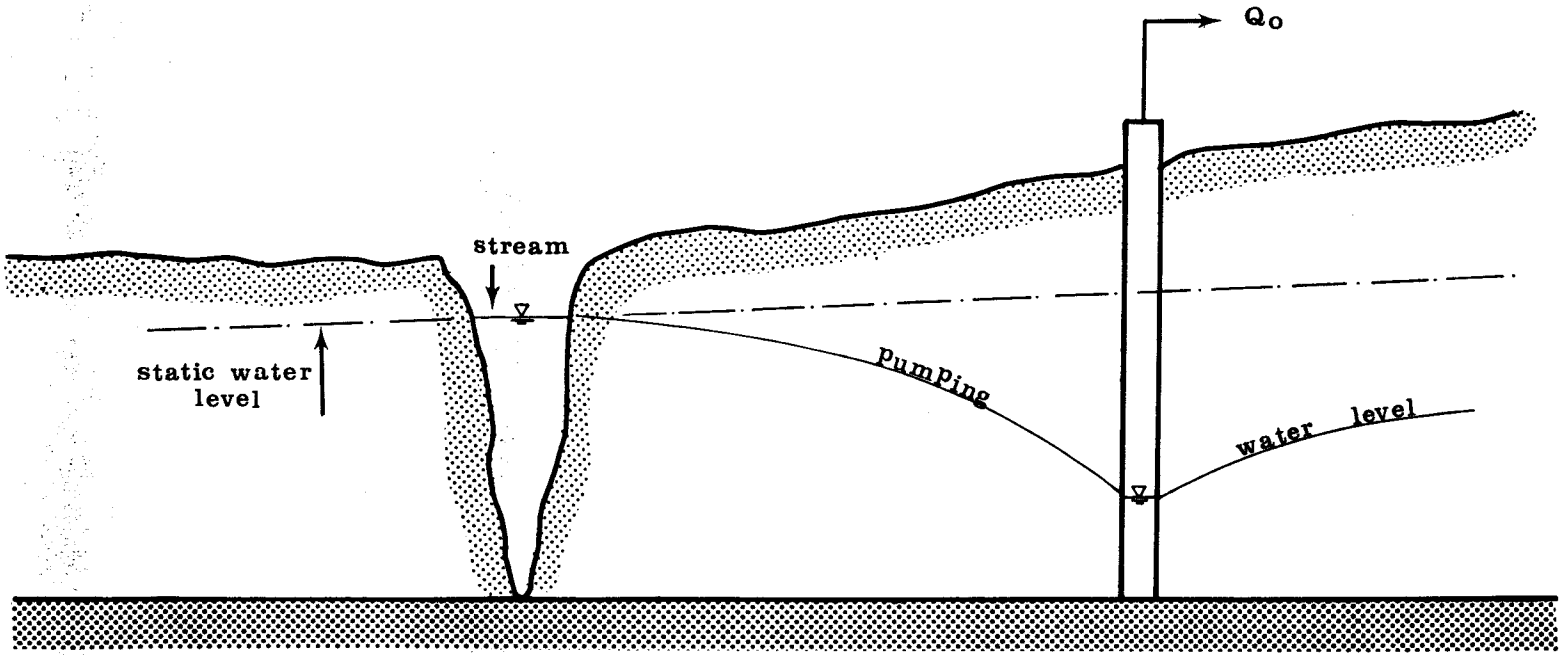

Figure 17

in which

$h(x,y,t)$ = potentiometric head

Q = pumping rate

T = transmissivity

$W(u^2)$ = logarithmic integral

$u^2 = \frac{S\, r^2}{4Tt}$

r_r = distance from a certain point to the real well (see Fig. 18)

r_i = distance from a certain point to the imaginary well (see Fig. 18)

The rate of infiltration from the stream into the aquifer per unit length of the stream is

$$q = T \cdot I$$

in which I is the gradient of the potentiometric surface normal to the stream. At a certain point along the stream $(0,y_o)$ the gradient I_r caused by the real well is given by (Fig. 18)

$$|I_r| = \left|\frac{\partial s_r}{\partial r}\right| = \frac{Q}{2\pi T}(a^2 + y_o^2)^{1/2}\exp[-(a^2 + y_o^2)S/4Tt]$$

in which a is the distance from the real well to the stream. The gradient caused by the imaginary well has the same magnitude.

Figure 18. Scheme of the imaginary well method.

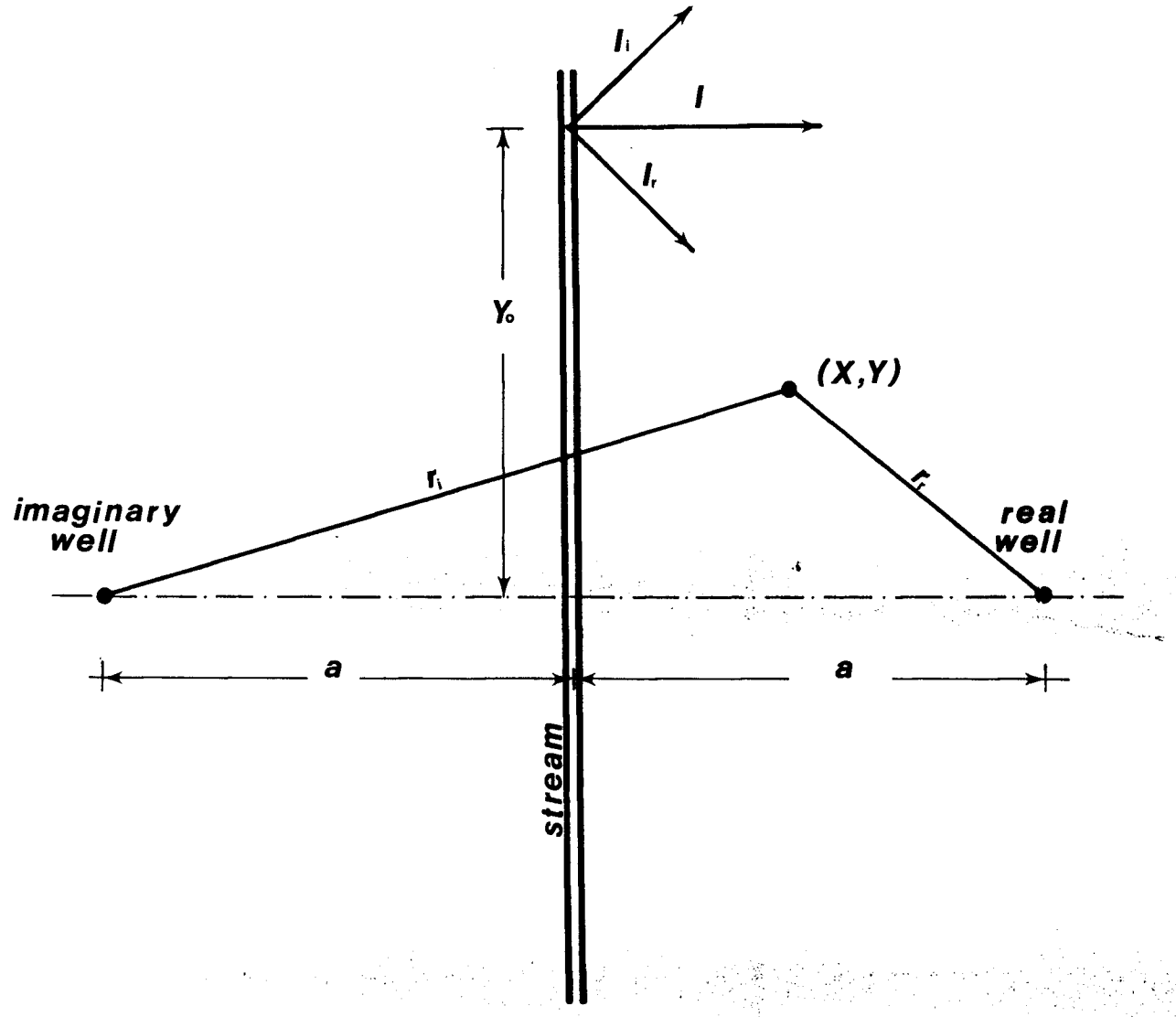

Figure 18

By vectorial addition of the two gradients, the resultant gradient perpendicular to the stream is

$$I = 2\left[\frac{Q}{2\pi T}(a^2 + y_o^2)^{-1/2}\exp[-(a^2 + y_o^2)S/4Tt] \cdot \right.$$

$$a(a^2 + y_o^2)^{-1/2} = \frac{Q}{\pi T}\frac{a}{a^2 + y_o^2}\exp\left[-(a^2 + y_o^2)S/4Tt\right]$$

Figure 19 shows the finite difference network, which for simplicity was desigined as a rectangular mesh. The aquifer parameters used for calculations where T = 20 m^2/day, S = 0.001. The well of a diameter 0.5 m was located 100 m from the stream, and pumped the water at a rate Q_o = 40 m^3/day.

The results of two numerical simulations, without and with modeling the properties of the radial flow, are shown in Figures 21 and 22, respectively. these results were obtained for two days of pumping. It may be seen that the correction for radial flow substantially improves accuracy of the results in the vicinity of the well.

Figure 22 shows the distribution of infiltration rate q along the stream, obtained from analytical and numerical solution. the numerical solution gives a stepwise function, which is a result of the assumption of constant value of all properties within the area surrounding each node. Thus, the numerical and analytical results differ locally. However, the difference between the integrals of these distributions over the stream length was relatively small, about 2%. That indicates the feasibility of the numerical method to simulate stream-aquifer interactions.

Figure 19. Finite difference mesh.

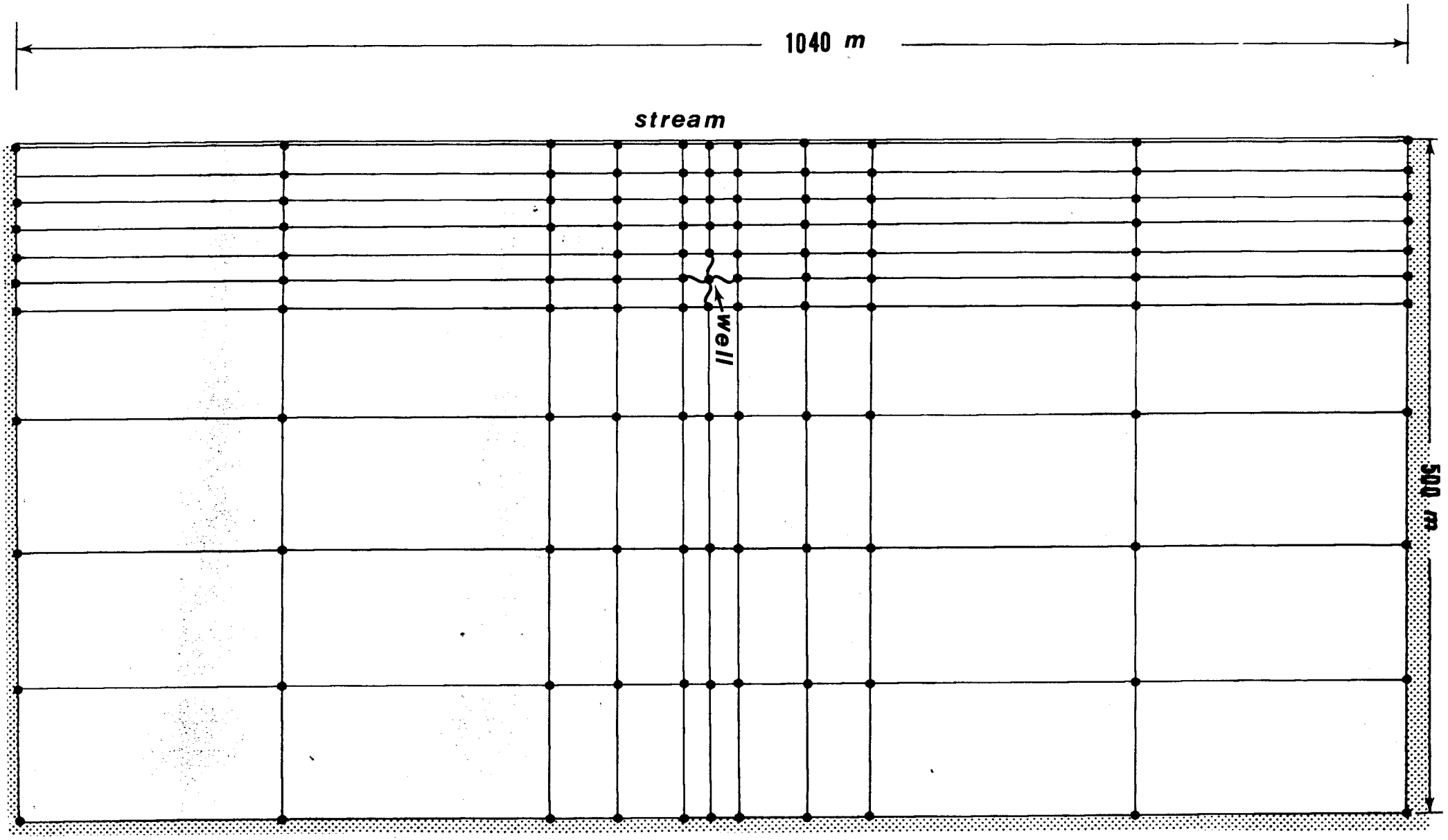

Figure 19

Figure 20. Drawdown calculated without modeling radial flow.

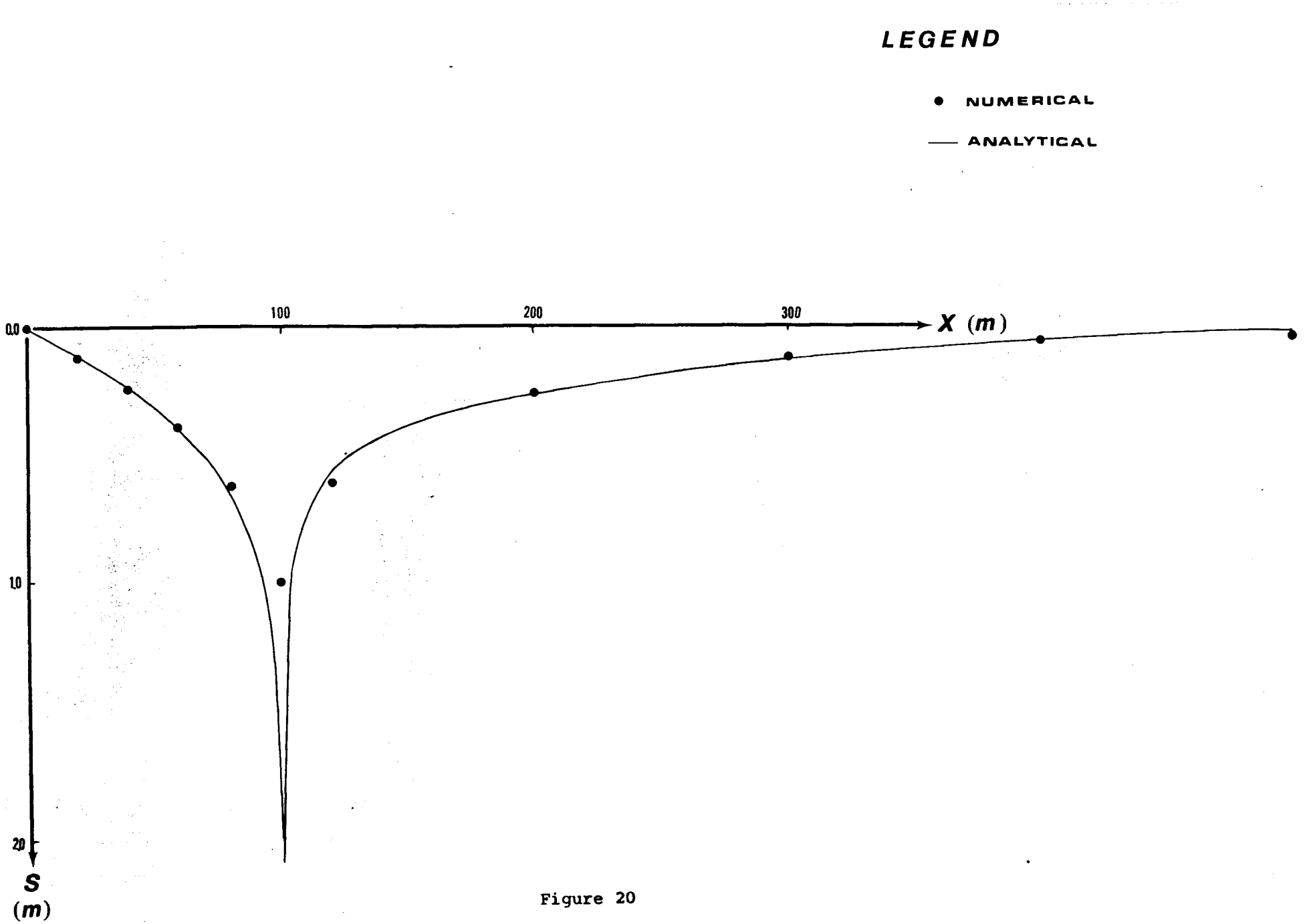

Figure 20

Figure 21. Drawdown calculated with modeling radial flow.

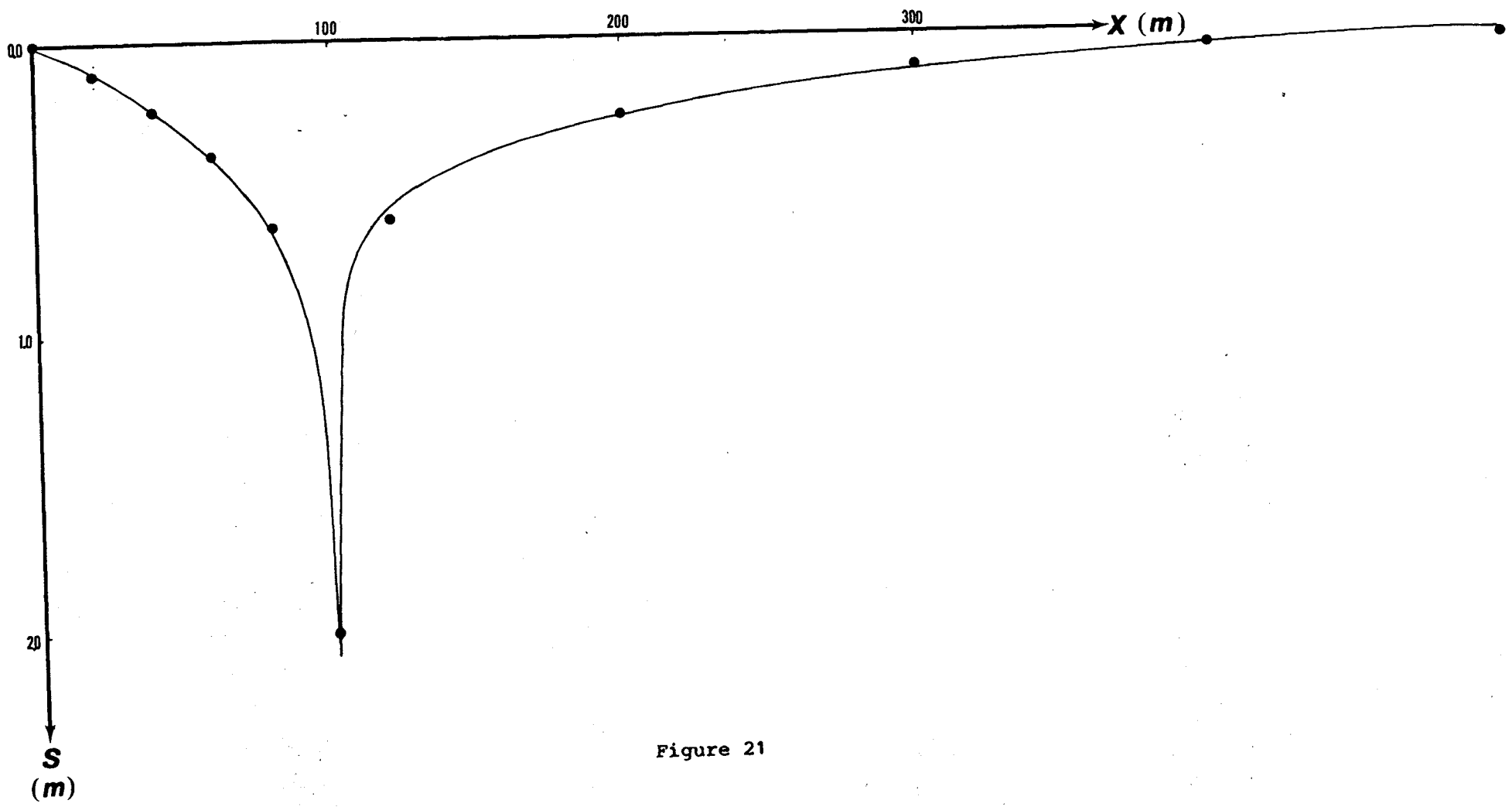

Figure 21

Figure 22. Infiltration rate distribution along the stream.

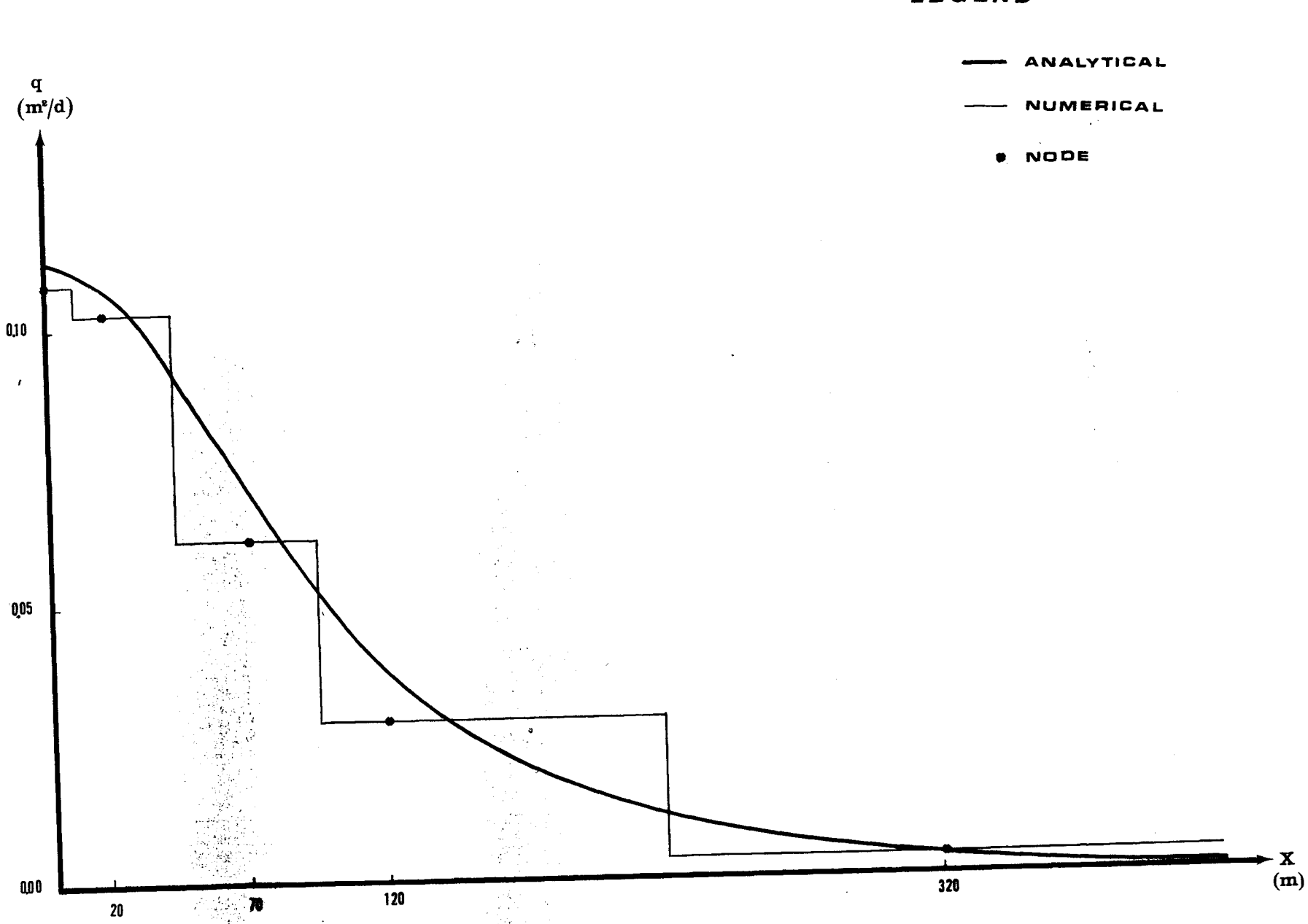
LEGEND
ANALYTICAL
NUMERICAL
NODE
q
(m²/d)
0.10
0.05
0.00
20
70
120
320
X
(m)

Figure 22

REFERENCES

Bear, J., 1972, Dynamics of fluids in porous media: New York, Elsevier, 764 p.

Chow, V.T., 1959, Open-channel hydraulics: New York, McGraw-Hill, 680 p.

Huisman, L., 1972, Groundwater recovery: New York, Winchester Press.

Kemblowski, M., Mioduszewski, W., 1978, Numerical calculation of subirrigations: Proceedings of X Congress of I.C.I.D., Athene, pp. 35.167-35.174.

Macneal, R.H., 1953, An asymmetrical finite difference network: Quarterly Applied Mathematics, vol. XI, no. 3, pp. 295-310.

Macon, N., 1963, Numerical analysis: New York, John Wiley, 161 p.

Rovey, C., 1975, Numerical model of flow in a stream-aquifer system: Colorado State University Hydrology Paper 74, 73 p.

Shestakov, V.M., 1965, Teoreticheskie osnovy otsenki podpora, vodoponizneniya i drenazha (Theoretical basis of assessing bank storage, pumping and drainage): Moscow, Izdat, MGU.

Walton, W.C., 1970, Groundwater resources evaluation: New York, McGraw-Hill, 664 p.

Kansas Geological Survey
Open-file Report

Disclaimer

The Kansas Geological Survey does not guarantee this document to be free from errors or inaccuracies and disclaims any responsibility or liability for interpretations based on data used in the production of this document or decisions based thereon. This report is intended to make results of research available at the earliest possible date, but is not intended to constitute final or formal publication.